Implementation and Evaluation of Automatic Contour Propagation in 4DCT of Lung

V. Boldea and G. Sharp and S. Jiang and N. Choi and C. Ginestet and C. Carrie and D. Sarrut

1. Introduction

Although 4D-CT promises to improve target delineation in patients with mobile tumors, it is difficult and time consuming to process the large amounts of data that are produced. For example, to generate an ITV, it is sometimes necessary to manually contour the target in multiple breathing phases. This project intends to improve clinical throughput by using deformable registration to propagate a manually drawn reference contour to other phases in the 4D-CT.

2. Material

4D-CT was acquired using a 4-slice GE light speed scanner and Varian RPM system. Scans were acquired in cine mode with 0.8 second rotation speed, and cine durations between 4 and 6 seconds at each couch position. By selecting appropriate images at each couch position, 10 complete CT volumes were obtained (a total of 880 slices). For validation purposes, GTV target volumes were manually contoured in the axial plane by a physician on all 10 phases of respiration.

3. Method

a) Deformable registration

We considered the end-exhale image as reference for the deformable registration. We computed deformable registration end-exhale image and the other 3D-CT images of the 4D-CT. We used a “demons” based algorithm with Gaussian regularization. Computation times ranged from less than 4 min. to about 10 min. according to the deformation amplitude (Pentium 4 2.8Gz, 1GiB Ram).

b) GTV Evaluation

Usually, the GTV is contoured on one reference phase (end-exhale for example) of the 4D-CT which is copied and edited on the others phases. This is a very important, but time consuming task that is inconvenient for every day clinical use. Using a deformation field computed between 4D-CT phases could accelerate the contouring process. The reference GTV contour would be deformed from one phase to another and the clinician would have to do only small adjustments. The contouring time spent would be significantly reduced. The question is if deformable registration could be used as a semi-automatic contouring tool.

To answer this question, we compared differences between GTV reported with and without deformation from one 4D-CT phases to another. We based our evaluation on three criterions to compare GTV volumes.

Let V_X, V_y be the GTV volumes of the images I_X and I_y (X≠Y) of the 4D-CT. The two volumes were superimposed on a same reference (for example, the image I_X). The first criterion is the volume intersection $V_X \cap V_y$ estimated by computing the number of voxels commons to the two volumes. The figure below illustrates an example of the superposition of two GTV of the end-inhale and end-exhale phases of the 4D-CT.

We used these criteria to compare V_X *to* V_y *and* V_y *to* V'_x, where V'_x the GTV of I_x automatically propagated by the deformation field computed between I_x and I_y**.** The new position p' in V'_x of each point p in V_x, was obtained by applying the computed displacement vector to p.

We also propose two other criterion. We evaluate the percentage of points belonging to volumes differences $V_y \setminus V'_x$ and $V'_X \setminus V_y$. If we consider V_y the reference GTV volume, the volume $V_y \setminus V'_X$ can be viewed as the volume planned for irradiation by the physicist but excluded from the GTV computed with deformable registration. Similarly, $V'_X \setminus V_y$ can be viewed as the volume which would be irradiated by the propagated GTV, but not by the physician's specifications.

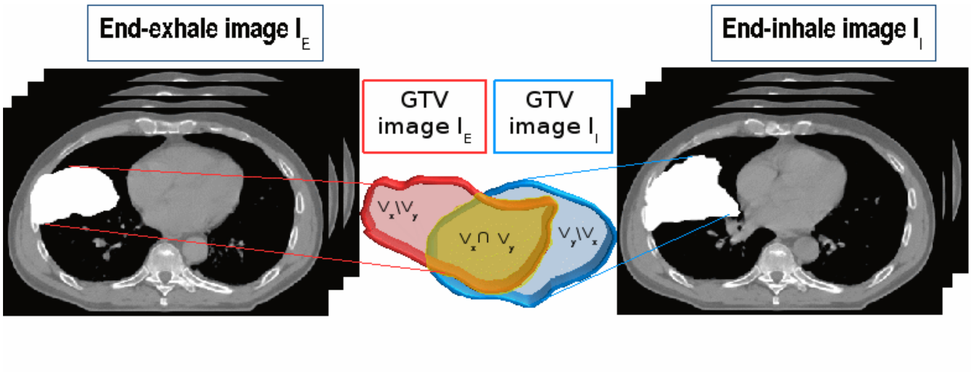

4. Results

The following table shows the volume intersection and difference values obtained with and without deformable registration. The GTV volume V_6 of the end-exhale image I_6 was used as the reference. Each row shows the volume intersection and differences when V_6 is propagated to another phase. The values are expressed in percentage of the reference volume V_6.

We observed a maximum difference of 28cm³ between the GTV volumes of the different phases of the 4D-CT. This corresponds to 9% of the GTV volume of the end-exhale 3D-CT image. If we compare this value against the contouring variability for the same expert from one image to another, we note that the volumes intersections with deformable registration are of the same order with a margin of 2% - 3%. We also note that for greater differences between GTV volumes ($V_6 - V_4$, $V_{10} - V_6$), we had also greater differences (about 15%) between volumes planned for irradiation by the physician and volumes obtained with deformable registration. This may be due to an approximate (not perfect) delineation of the GTV and/or to a bad deformable registration locally.

	V_X	V_6	Without D-R (%)				With D-R (%)			
Vol.	(cm^3)	(cm^3)	$V_X \cap V_6$	$\frac{V_X \setminus V_6}{V_6}$	$\frac{V_6 \setminus V_X}{V_6}$	$\frac{V_X \cap V_6}{V_X \cup V_6}$	$V'_X \cap V_6$	$\frac{V'_X \setminus V_6}{V_6}$	$\frac{V_6 \setminus V'_X}{V_6}$	$\frac{V'_X \cap V_6}{V'_X \cup V_6}$
$V_5 - V_6$	313.8	302.0	93.5	6.5	10.4	84.7	92.7	7.3	11.2	84.0
$V_4 - V_6$	323.6	302.0	89.6	10.4	17.6	76.2	91.1	8.9	16.1	78.0
$V_3 - V_6$	311.5	302.0	79.2	20.8	23.9	63.9	87.5	12.5	15.7	75.0
$V_2 - V_6$	302.2	302.0	71.2	28.8	28.9	55.2	85.8	14.2	14.3	73.2
$V_1 - V_6$	299.3	302.0	69.7	30.3	29.4	53.9	85.5	14.5	13.6	74.5
$V_{10} - V_6$	325.9	302.0	76.9	23.1	31.1	58.7	90.1	9.9	17.8	77.3
$V_9 - V_6$	304.7	302.0	93.6	6.4	7.3	87.3	90.2	9.8	10.7	78.3
$V_8 - V_6$	297.7	302.0	93.4	6.6	5.2	88.9	90.0	10.0	8.5	81.0
Mean	309.8	302.0	83.4	16.6	19.2	71.1	89.1	10.9	13.5	77.7

5. Conclusion

These preliminary results showed that deformable registration may be useful for a semi-automatic contouring tool appropriate for every day clinical use. If the registration has been performed off-line, the contours propagation can be executed quickly. Thus, deformation vector fields can be used to automatically propagate GTV contours delineated in a reference 3D-CT (end-exhale) to the others 3D-CT of the 4D-CT acquisition.